

## Supporting Information

### Removal of the X-ray contrast media diatrizoate by electrochemical reduction and oxidation

Jelena Radjenovic<sup>1,\*</sup>, Victoria Flexer<sup>1</sup>, Bogdan C. Donose<sup>1</sup>, David L. Sedlak<sup>2</sup>, Jurg Keller<sup>1</sup>

<sup>1</sup>Advanced Water Management Centre, The University of Queensland, QLD 4072, Australia

<sup>2</sup>Department of Civil and Environmental Engineering, University of California, Berkeley, CA  
94720-1710, USA

Number of pages: 28

Number of tables: 3

Number of figures: 19

\*corresponding author

Dr Jelena Radjenovic

Phone: +61 7 3346 3233,

Fax: +61 7 3365 4726,

e-mail: [j.radjenovic@awmc.uq.edu.au](mailto:j.radjenovic@awmc.uq.edu.au)

**Text S1** Chemicals

All solutions were prepared using analytical grade reagents and Milli-Q water. Analytical standards for sodium diatrizoate dihydrate and 3,5-diacetamidobenzoic acid were purchased from Sigma-Aldrich (Steinheim, Germany). Potassium phosphate monobasic ( $\text{KH}_2\text{PO}_4$ ), potassium phosphate dibasic ( $\text{K}_2\text{HPO}_4$ ), sodium chloride ( $\text{NaCl}$ ) and potassium hydroxide ( $\text{KOH}$ ) were purchased from Ajax Finechem (Auckland, New Zealand). Solvents for liquid chromatography were purchased from Merck (Darmstadt, Germany).

**Text S2** Preparation of Pd nanoparticles-loaded graphite felt electrodes

Polyelectrolyte self-assembled multilayers (PEMs) were formed by alternate immersion in polyallylamine (PAH, 15mM, pH 8) and polyacrylic acid (PAA, 15mM, pH 4) solutions for 30 minutes, starting from PAH, with 200 RPM magnetic stirring. Between adsorption steps, electrodes were washed twice in reverse osmosis water for 15 min. 5 layers were self-assembled: PAH/PAA/PAH/PAA/PAH. The samples were then soaked in 1 mM  $\text{PdCl}_4^{2-}$  (in 0.1 M KCl, pH 2.5) solution for 24 h and thoroughly rinsed with water. The confined  $[\text{PdCl}_4]^{2-}$  ions were potentiostatically reduced at -500 mV vs Ag/AgCl in a  $\text{H}_2\text{SO}_4$  0.1 M solution for 12 minutes. A positively charged capping layer (PAH) in multilayers films facilitates the adsorption of the negatively charged Pd ions ( $\text{PdCl}_4^{2-}$ ). The  $\text{PdCl}_4^{2-}$  exchange/reduction step was repeated a second time.

Scanning Electron Microscope (SEM) imaging (secondary electrons) was performed on a Field Emission Jeol JSM-7001F microscope with a hot (Schottky) electron gun operated at 15 kV. Energy dispersive X-ray spectroscopy (EDS) measurements were performed on a XL30 Philips (LaB6 source electron gun) Scanning Electron Microscope, operated at an accelerating voltage of 20 kV. Elemental analysis was performed in spot measurement mode at 60 s integration time.

**Text S3** Palladium nanoparticle characterization.

The Pd electrochemically active area was estimated from the reduction peak of palladium oxide (Figure S4), using a relationship of  $420 \mu\text{C cm}^{-2}$ . A Pd-NP size distribution histogram (see Figure S5) was obtained employing the Particle Analysis module of the Scanning Probe Image Processor (Image Metrology) V 5.0.7 on an QLD Node-Australian National Fabrication Facility Licence. Typically, SEM micrographs were flattened and XY calibrated, followed by manually setting an intensity threshold and automatic particle detection. Particles with radii below 3 nm and above 100nm were trimmed from histograms (80 bins) as corresponding to surface noise and non-Pd aggregates.

**Text S4** UFLC-QLIT-MS analysis of diatrizoate and its reduction products.

Diatrizoate and its reduction by-products DTR-I (3,5-diacetamido-diiodobenzoic acid), DTR-2I (3,5-diacetamido-iodibenzoic acid), and DTR-3I (3,5-diacetamidobenzoic acid) were analysed in positive electrospray ((+)ESI) mode. Eluent A was acetonitrile with 0.1% formic acid, and eluent B was HPLC grade water with 0.1% formic acid. The elution gradient started with 5% eluent A, increasing to 20% in 10 min, raising to 50% in the following 5 min, further increasing to 100% of A in the next 3 min. Next, the gradient was isocratically held at 100% of A for 4 min before returning to the initial conditions and re-equilibrating the column for 4 min. Chromatographic analysis was complete after 26 min. Chromatographic separation was achieved with an Alltima C18 Column (250 × 4.6 mm, particle size 5 µm) run at 40 °C, from Alltech Associates Inc. (Deerfield, IL, U.S.A.).

The optimized compound dependent MS parameters (declustering potential (DP), collision energy (CE) and cell exit potential (CXP)) for each transition are summarized in Table S1. Settings for source-dependent parameters were as follows: curtain gas (CUR), 30V; nitrogen collision gas (CAD) high; source temperature (TEM) was 700 °C; ion source gases GS1 and GS2 were set at 62V; ion spray voltage was set at 5500V.

## Text S5

In the experiments performed in batch mode, electrolysis time was calculated as a ratio of the cathodic compartment volume ( $V_{CAT}$ , L) or anodic compartment volume ( $V_{AN}$ , L), and total volume ( $V$ , L), and multiplied by the real experiment time (Eq 1):

$$t_{el} = \frac{V_{CAT}}{V} * t = \frac{V_{AN}}{V} * t \quad (\text{Eq 1}).$$

Theoretical release of iodide ions ( $c_{I,theor}$ ,  $\text{mg L}^{-1}$ ) was calculated as the maximum possible release of I for a given experiment, assuming that the decrease in diatrizoate concentration corresponded to its complete deiodination (Eq 2):

$$c_{I,theor} = (c_{DTR,0} - c_{DTR}) * \frac{3 * MW_I}{MW_{DTR}} \quad (\text{Eq 2}),$$

where  $c_{DTR,0}$  and  $c_{DTR}$  are the initial and concentration ( $\text{mg L}^{-1}$ ) of diatrizoate at time  $t$ , respectively, and  $MW_I$  and  $MW_{DTR}$  are molecular weights of iodine and diatrizoate, respectively.

Diatrizoate removal efficiency ( $Ef_{DTR}$ , %) was calculated using the following equation:

$$Ef_{DTR} = \frac{c_{DTR,0} - c_{DTR}}{c_{DTR,0}} * 100\% \quad (\text{Eq 3}).$$

Deiodination efficiency ( $Ef_I$ , %) was calculated as a percentage ratio of experimentally determined concentration of iodide ions ( $c_{I,exp}$ ,  $\text{mg L}^{-1}$ ) and  $c_{I,theor}$  (Eq 4):

$$Ef_I = \frac{c_{I,exp}}{c_{I,theor}} * 100\% \quad (\text{Eq 4}).$$

In electrochemical reduction in batch mode, Coulombic efficiency of diatrizoate deiodination was calculated with respect to the cathodic compartment volume as follows:

$$\varepsilon = \frac{2 * V_{CAT} * F * C_I}{I * t} \quad (\text{Eq 5}),$$

where 2 is the number moles of electrons per mole of iodide ion released,  $F$  is Faraday's constant ( $96485 \text{ C mol}^{-1} \text{ e}$ ),  $C_I$  is the concentration of iodide ions measured at time  $t$  ( $\text{mol L}^{-1}$ ),  $I$  is the measured cathodic current, and  $t$  is time.

The energy ( $E$ ,  $\text{kWh m}^{-3}$ ) used in a coupled reductive and oxidative electrochemical treatment in continuous mode was calculated with respect to the cathodic flow rate ( $Q_C$ ), cathodic current ( $I_{CAT}$ ), and total cell potential ( $E_{TOT}$ ) as follows:

$$E = \frac{E_{TOT} * I_{CAT}}{Q_C} \quad (\text{Eq 6}).$$

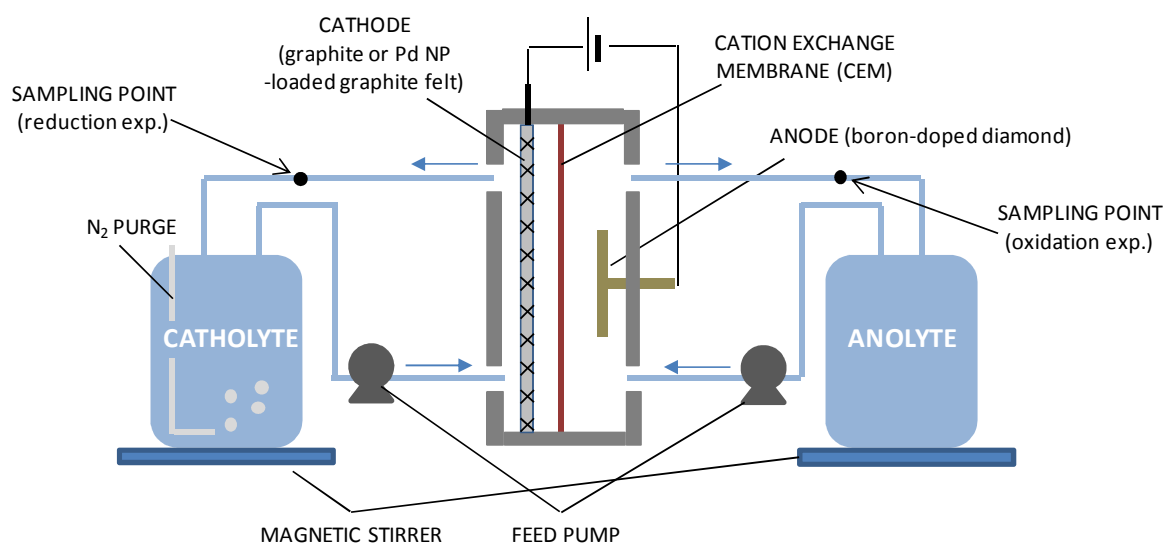


**Figure S1** Scheme of the divided electrolytic cell used in electrochemical oxidation and reduction experiments.

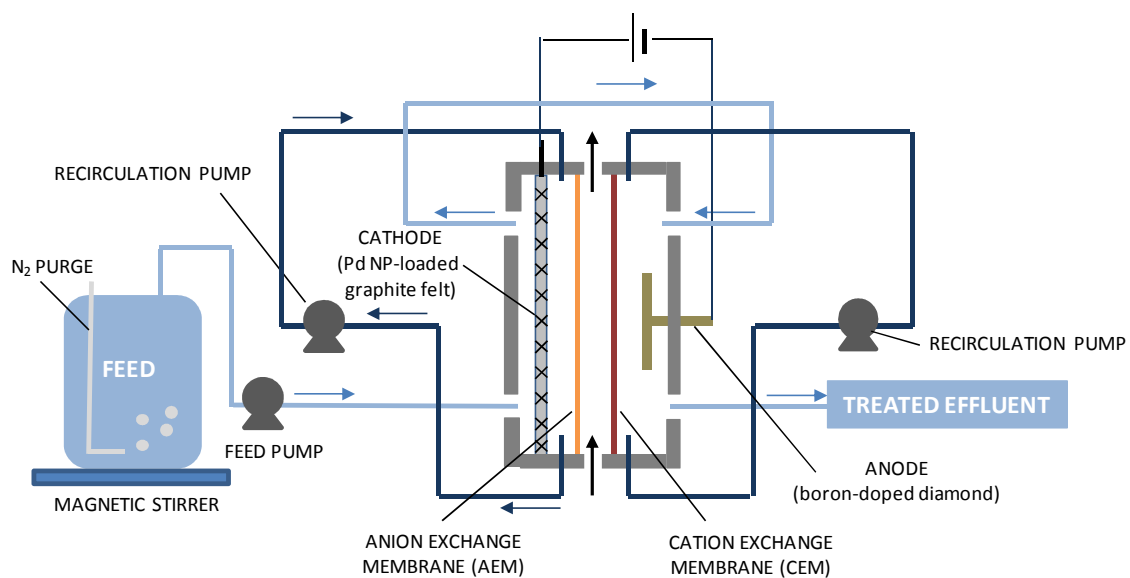


**Figure S2** Scheme of the three-compartment electrolytic cell used in combined electrochemical reduction and oxidation experiments.

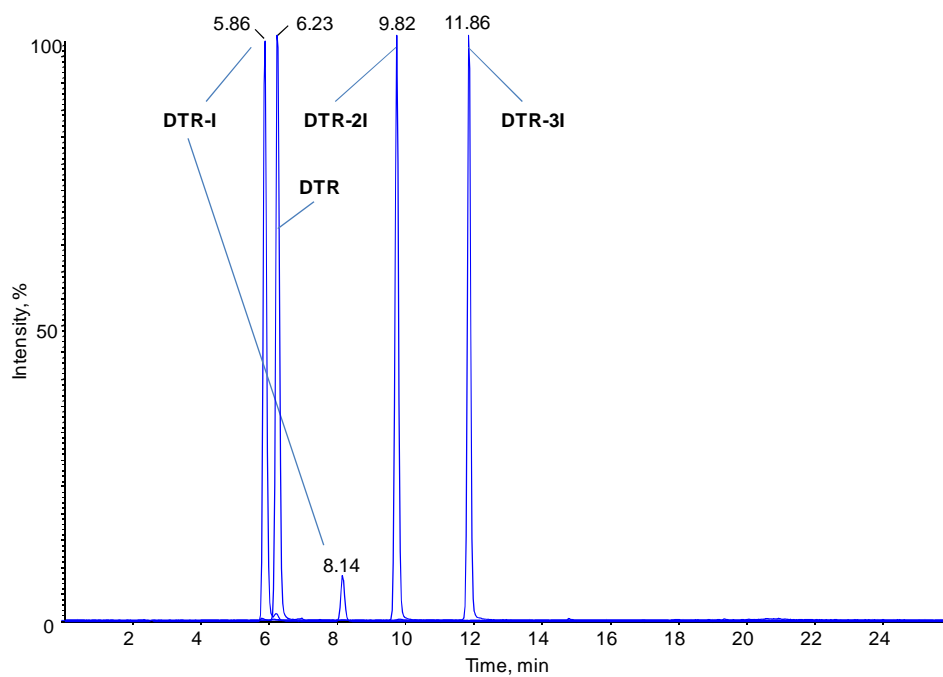


**Figure S3** Extracted ion chromatograms of diatrizoate and its reduction products recorded in the (+)ESI MRM mode.

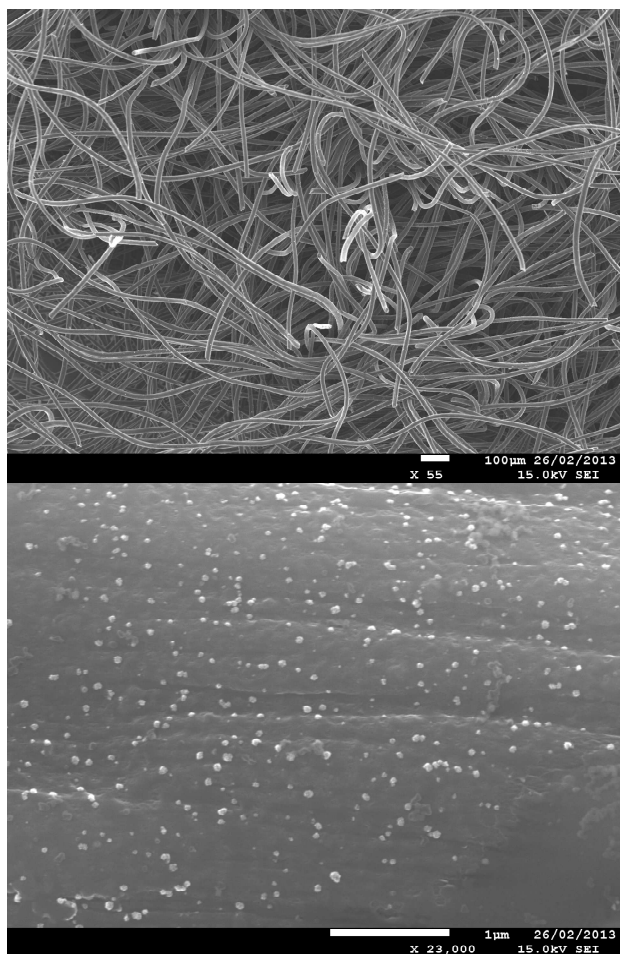


**Figure S4** Scanning electron micrographs (SEM) of graphite felt electrodes doped with Pd nanoparticles at different magnifications.

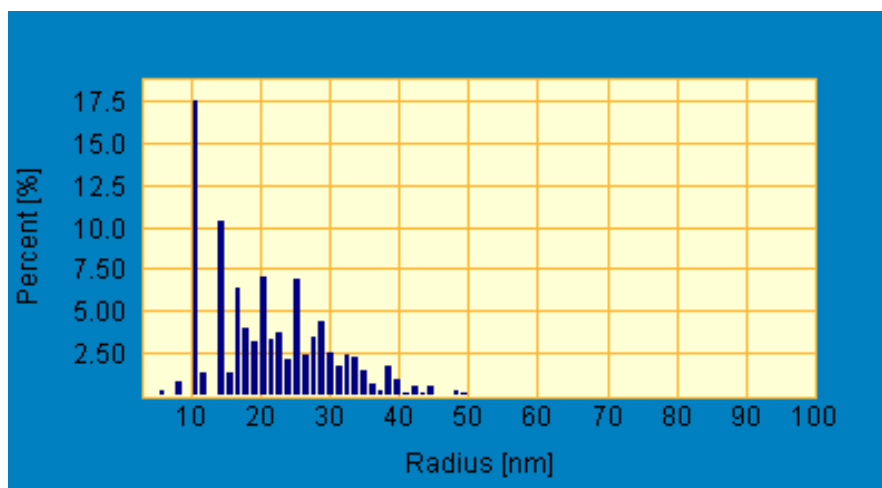


**Figure S5** Pd nanoparticle size distribution histogram obtained from Figure S4. Average radius 20 nm and a standard deviation 11 nm.

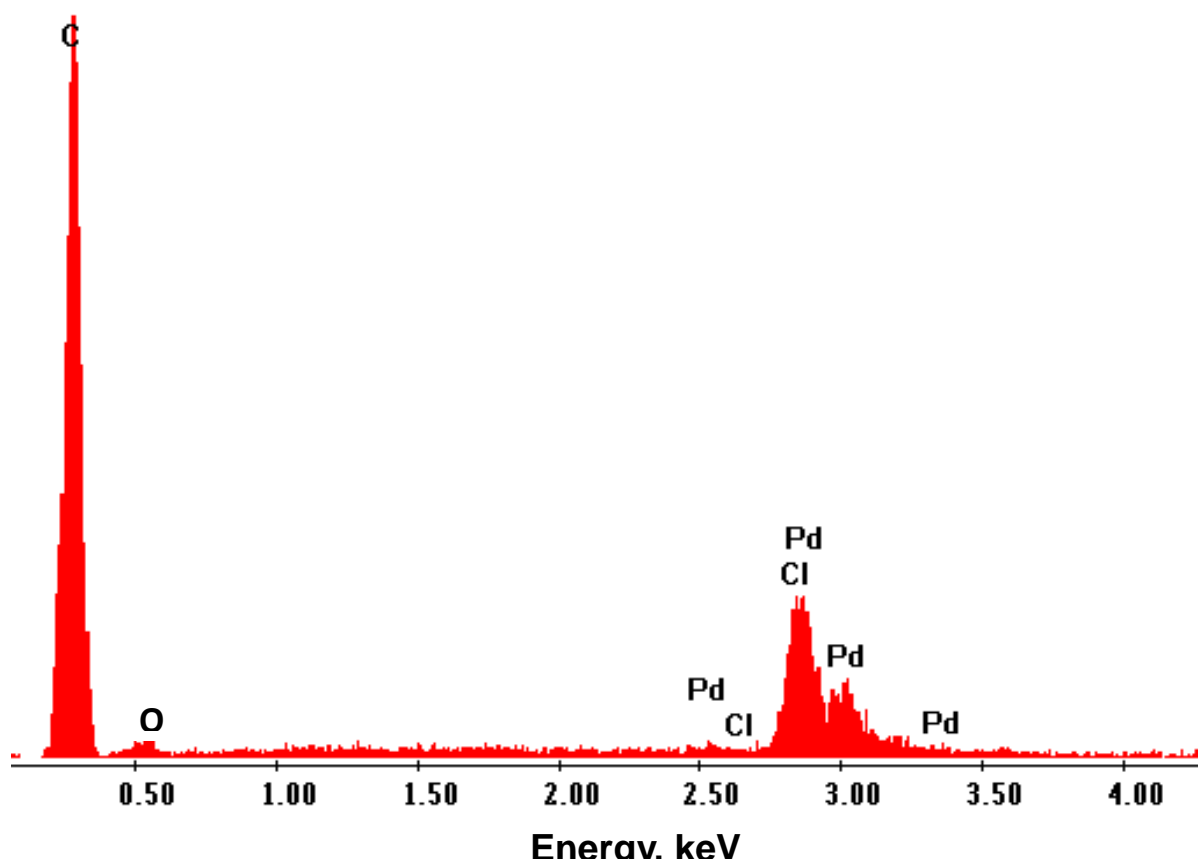


**Figure S6** Energy Dispersive X-ray Spectroscopy (EDS) spot profile of the as synthesised Pd nanoparticles on graphite felt electrode (20 kV accelerating voltage, 60s integration time).

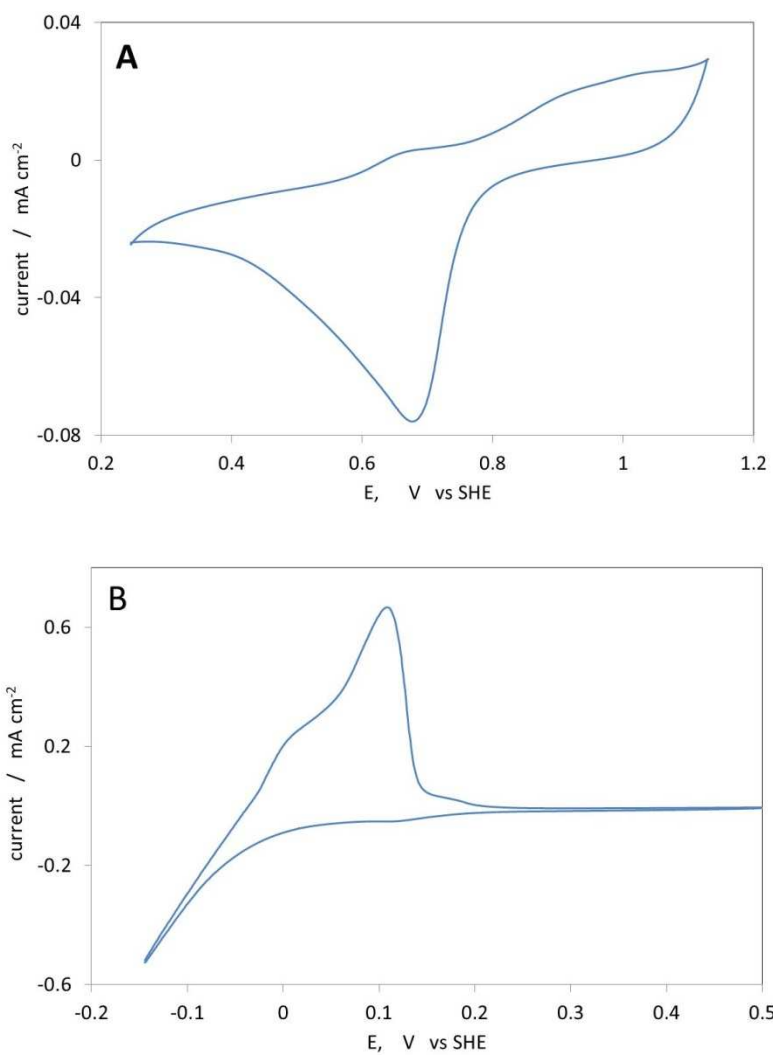


**Figure S7** Cyclic voltammograms for Pd nanoparticles-doped graphite felt electrodes: **A)** Pd oxide region, and **B)** H<sub>2</sub> adsorption region.

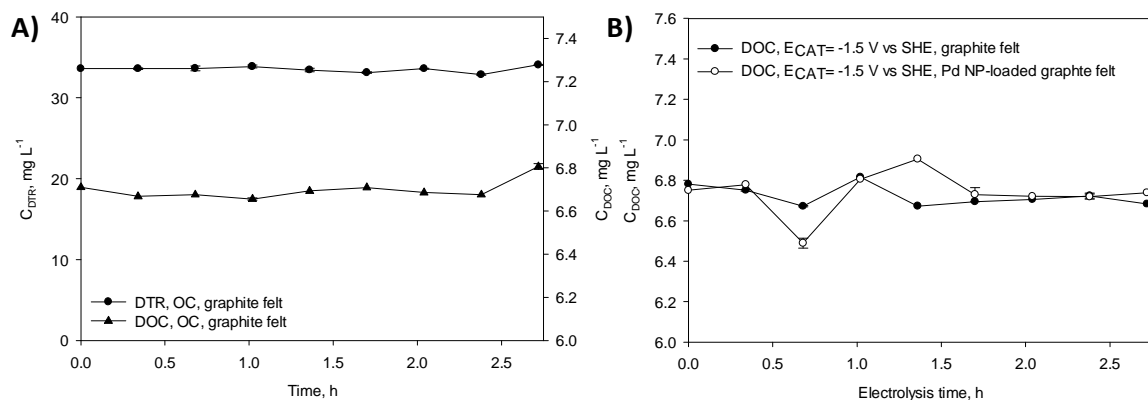


**Figure S8 A)** Concentration of diatrizoate and dissolved organic carbon (DOC) determined in the open circuit (OC) experiment using graphite felt cathode, and **B)** concentration of DOC determined in the electrochemical reduction of diatrizoate at graphite felt and Pd nanoparticles-loaded graphite felt at cathode potential ( $E_{CAT}$ ) of -1.5 V vs Standard Hydrogen Electrode (SHE). The initial concentration of diatrizoate was 50  $\mu\text{M}$ .

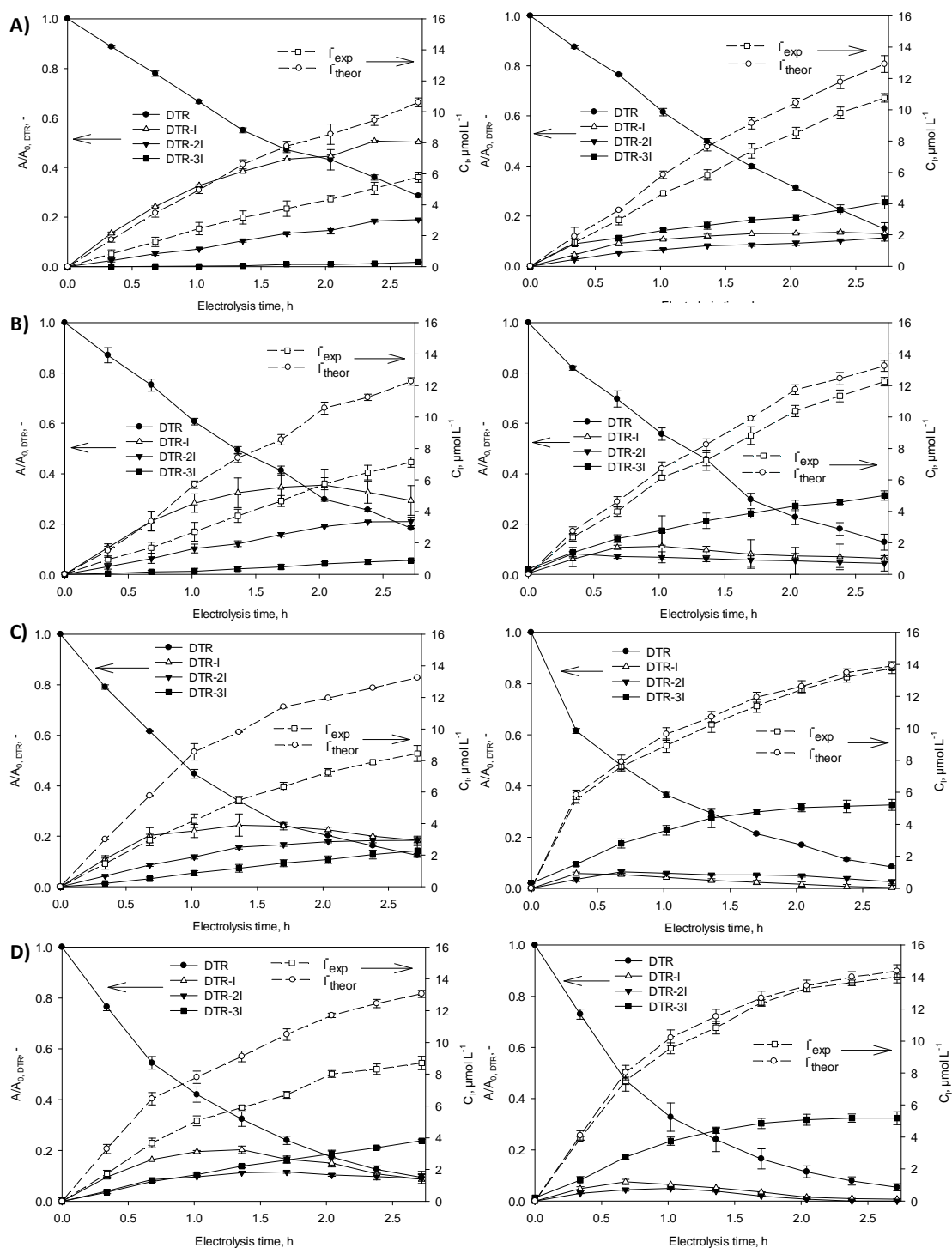


**Figure S9** Qualitative profiles of diatrizoate and its reduction products DTR-I (3,5-diacetamido-diiodobenzoic acid), DTR-2I (3,5-diacetamido-iodibenzoic acid), and DTR-3I (3,5-diacetamidobenzoic acid), obtained based on their relative areas to the initial area of diatrizoate ( $A_0$ ), is depicted on the left axis. Theoretical ( $\Gamma_{\text{theor}}$ ) and experimental ( $\Gamma_{\text{exp}}$ ) release of iodide in electroreduction at bare graphite felt (left) and Pd nanoparticles-loaded graphite felt (right), in phosphate buffer (pH 7.0) is depicted on the right axis, at  $E_{\text{CAT}}$ : **A)** -1.1 V vs SHE, **B)** -1.3 V vs SHE, **C)** -1.5 V vs SHE, and **D)** -1.7 V vs SHE. Values are expressed as means of two experiments, with their standard deviations.

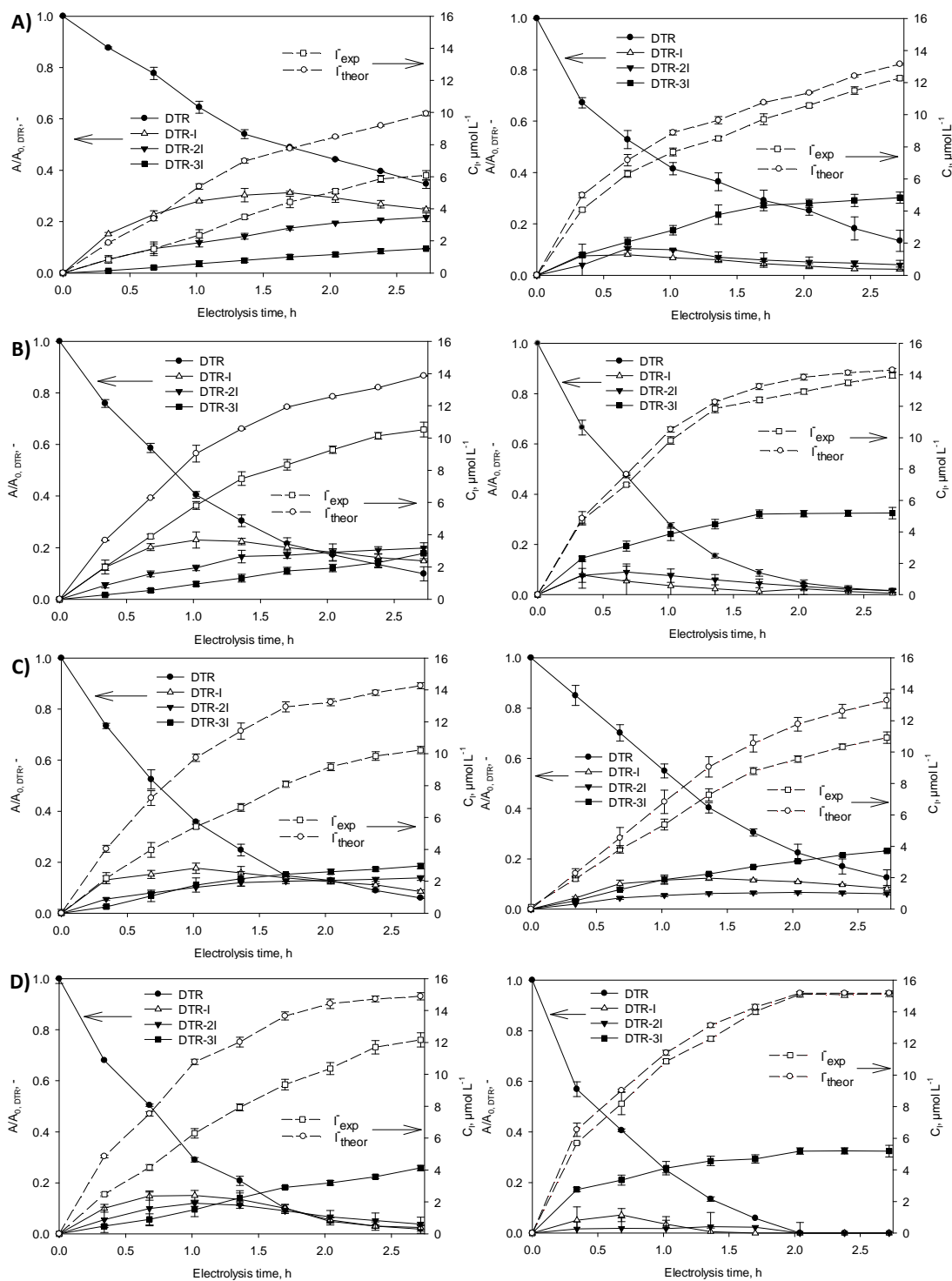


**Figure S10** Qualitative profiles of diatrizoate and its reduction products DTR-I, DTR-2I, and DTR-3I, obtained based on their relative areas to the initial area of diatrizoate ( $A_0$ ), is depicted on the left axis. Theoretical ( $\Gamma_{\text{theor}}$ ) and experimental ( $\Gamma_{\text{exp}}$ ) release of iodide in electroreduction of diatrizoate at  $E_{\text{CAT}} = -1.5$  V vs SHE at bare graphite felt (left) and Pd nanoparticles-loaded graphite felt (right), in phosphate buffer is depicted on the right axis: **A**) dissolved oxygen =  $7.2 \text{ mg L}^{-1}$ , **B**) addition of 10 mM NaCl, **C**) pH = 11, and **D**) cathodic flow rate ( $Q_C$ ) =  $200 \text{ mL min}^{-1}$ . Values are expressed as means of two experiments, with their standard deviations.

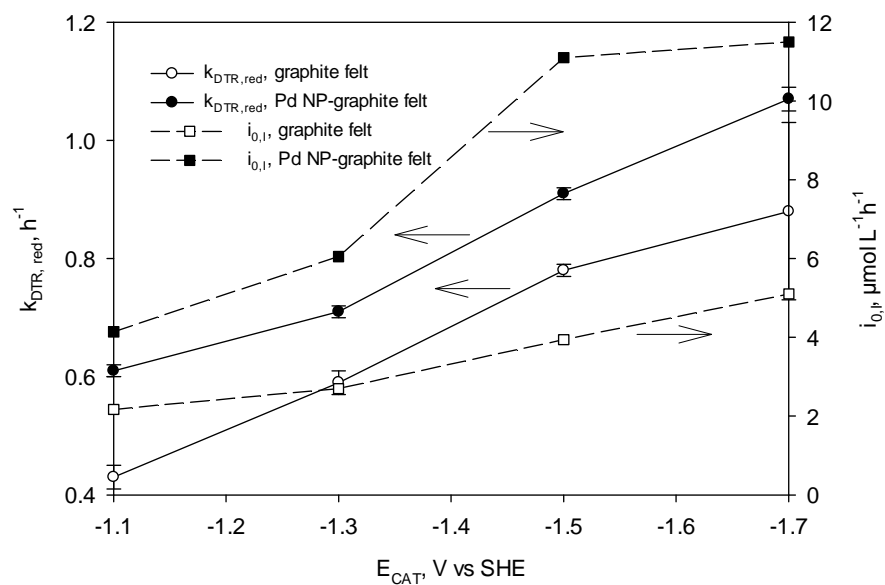


**Figure S11** First-order rate constants of diatrizoate reduction ( $k_{DTR,red}$ ,  $h^{-1}$ ) and initial rates of  $I^-$  release ( $i_{0,I}$ ,  $\mu mol L^{-1} h^{-1}$ ) vs applied  $E_{CAT}$  for graphite felt and Pd nanoparticles-loaded graphite felt. The initial rates of iodide release were calculated as the slope of the tangent line at  $t=0$  h of the curve of mean iodide ions concentration ( $I_{exp}$ ) versus electrolysis time.

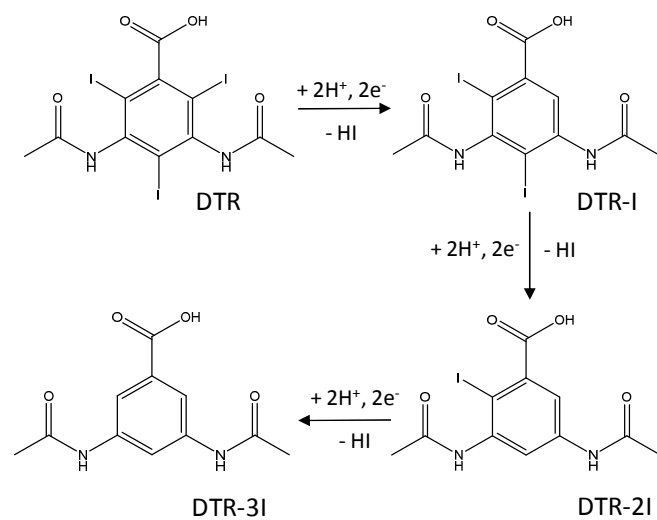


**Figure S12** Proposed pathway of diatrizoate (DTR) deiodination at graphite felt cathode. The exact position of the iodine release could not be determined. While the structures of the reduction products are accurate in terms of the number of remaining iodine atoms, they are not necessarily accurate with respect to their position on the aromatic ring.

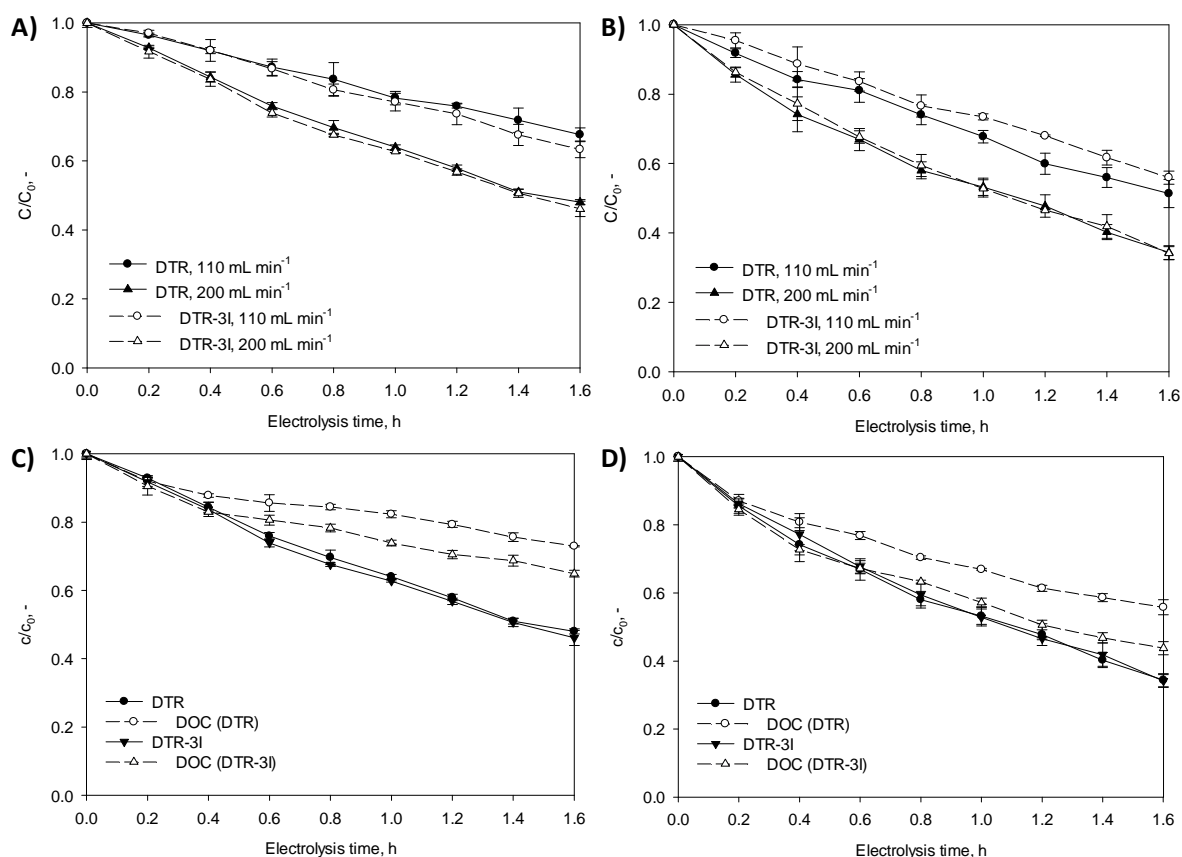


**Figure S13** Normalized concentrations of diatrizoate, DTR-3I, and DOC versus electrolysis time (h) in electrochemical oxidation at BDD anode at anode potential ( $E_{AN}$ )= +3.5 V vs SHE: **A)** 5  $\mu\text{M}$  diatrizoate and DTR-3I solution at pH 2.0, and **B)** 5  $\mu\text{M}$  diatrizoate and DTR-3I solution pH 7.0, **C)** 50  $\mu\text{M}$  diatrizoate and DTR-3I solution at pH 2.0, anodic flow rate ( $Q_A$ )=200 mL min<sup>-1</sup>;  $k_{DTR,ox}=0.460\pm 0.008$  h<sup>-1</sup>,  $k_{DTR-3I,ox}=0.481\pm 0.007$  h<sup>-1</sup>, and **D)** 50  $\mu\text{M}$  diatrizoate and DTR-3I solution at pH 7.0,  $Q_A=200$  mL min<sup>-1</sup>,  $k_{DTR,ox}=0.647\pm 0.004$  h<sup>-1</sup>,  $k_{DTR-3I,ox}=0.653\pm 0.006$  h<sup>-1</sup> ( $r^2 \geq 0.99$  in all cases).

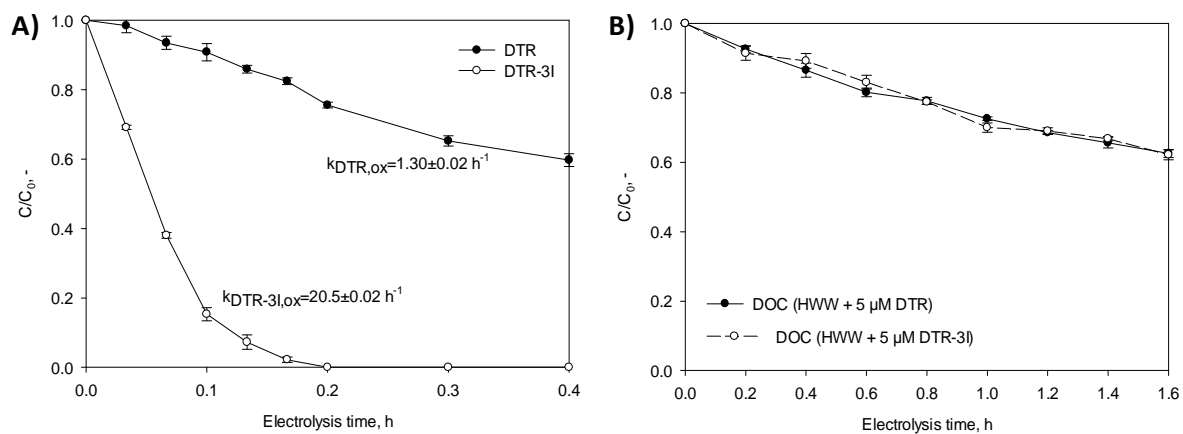


**Figure S14** A) Concentrations of diatrizoate and DTR-3I normalized to their initial values, and B) normalized DOC concentrations in electrochemical oxidation in hospital wastewater at  $E_{AN} = +3.5 \text{ V}$  vs SHE, pH 7.0 and  $Q_A = 110 \text{ mL min}^{-1}$ .

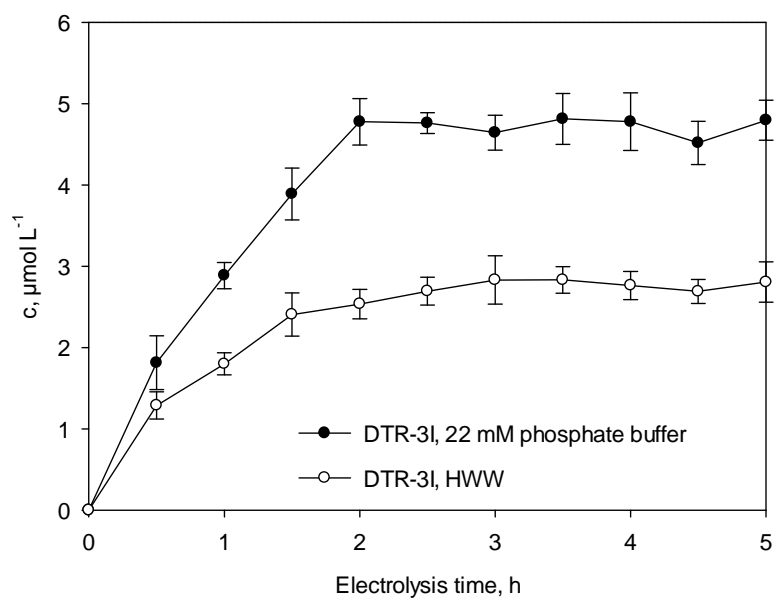


**Figure S15** Concentration of DTR-3I in the effluent of the cathodic compartment in combined electrochemical reduction and oxidation experiments in continuous mode and at  $E_{\text{CAT}} = -1.7 \text{ V vs SHE}$ , using 22 mM phosphate buffer and hospital wastewater (HWW). The buffer solution and hospital wastewater were amended with 5  $\mu\text{M}$  of diatrizoate. The samples batch of hospital wastewater already contained diatrizoate at a concentration of  $3.72 \pm 0.04 \text{ nM}$ .

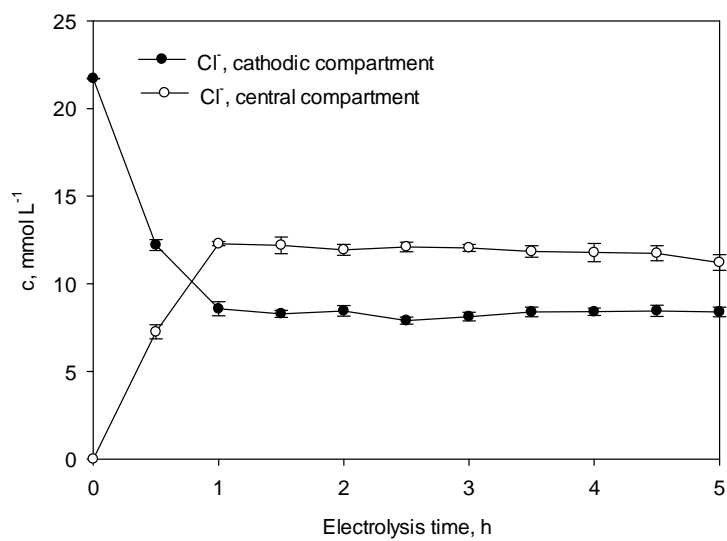


**Figure S16** Concentrations of chloride ions measured in the cathodic and central compartment of three-compartment electrolytic cell in combined electrochemical reduction ( $E_{\text{CAT}} = -1.7 \text{ V vs SHE}$ ) and oxidation ( $E_{\text{AN}} = 3.4\text{-}3.5 \text{ V vs SHE}$ ) of hospital wastewater in continuous mode.

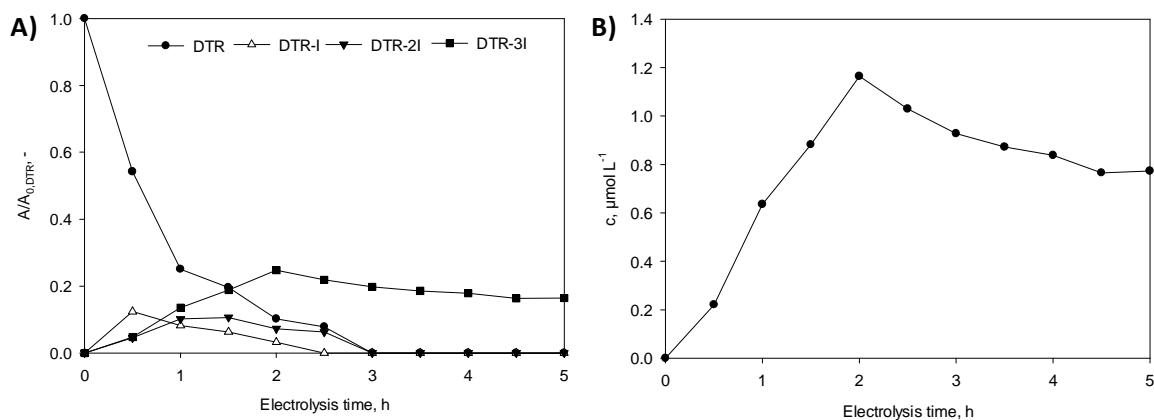


**Figure S17** Electrochemical oxidation at BDD at  $E_{AN} = +3.4-3.5$  V vs SHE, in continuous coupled electrochemical reduction and oxidation of  $5 \mu\text{M}$  solution of diatrizoate in  $22 \text{ mM}$  phosphate buffer (initial pH 7.0): **A)** qualitative profiles of diatrizoate and its reduction products DTR-I, DTR-2I and DTR-3I, obtained based on their relative areas to the initial area of diatrizoate ( $A_0$ ), and **B)** concentration of DTR-3I, measured in the effluent of the anodic compartment.

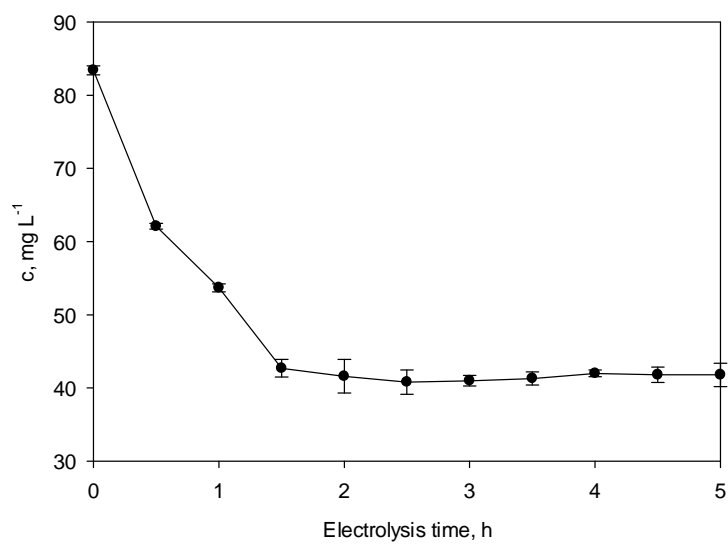


**Figure S18** Removal of DOC in anodic treatment of combined electrochemical reduction and oxidation of the hospital wastewater.

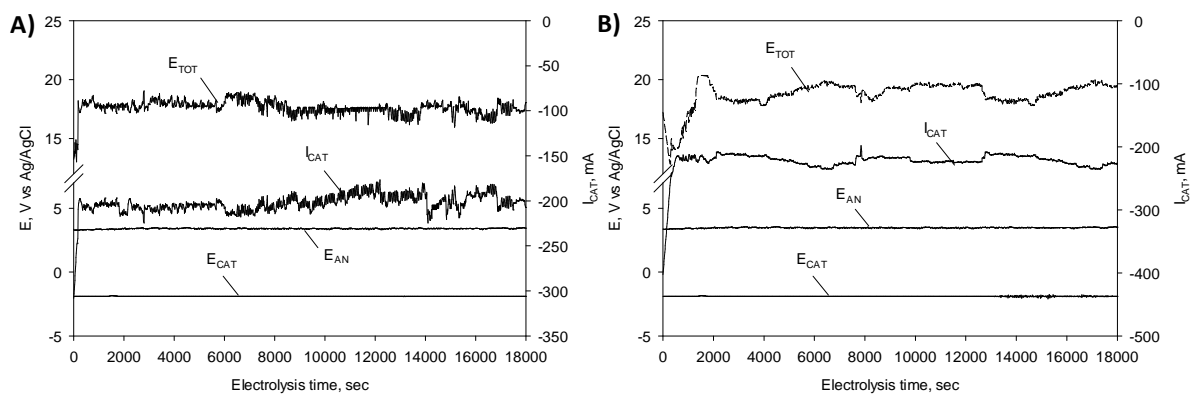


**Figure S19** Coupled electrochemical reduction and oxidation of 5  $\mu\text{M}$  solution of diatrizoate in: **A)** 22 mM phosphate buffer, and **B)** hospital wastewater; potential applied at Pd nanoparticles-loaded graphite felt ( $E_{\text{CAT}}$ , V), the resulting cathodic current ( $I_{\text{CAT}}$ , mA), total cell potential ( $E_{\text{TOT}}$ , V), and BDD anode potential ( $E_{\text{AN}}$ , V).

**Table S1** Method parameters applied in multiple reaction monitoring (MRM) mode in quadrupole linear ions trap mass spectrometry (QLIT-MS) analyses of diatrizoate and its reduction products DTR-I (3,5-diacetamido-diiodobenzoic acid), DTR-2I (3,5-diacetamido-iodibenzoic acid), and DTR-3I (3,5-diacetamidobenzoic acid), in (+)ESI mode. DP-declustering potential, CE-collision energy, CXP-cell exit potential, SRM

<b>Compound</b>	<b>Precursor ion, m/z</b>	<b>MRM 1</b>	<b>DP-CE-CXP (V)</b>	<b>MRM 2</b>	<b>DP-CE-CXP (V)</b>	<b>t<sub>R</sub>, min</b>
<b>DTR</b>	615.0	361.0	80-30-10	233.1	85-33-10	6.2
<b>DTR-I</b>	489.0	235.1	75-35-10			5.9; 8.1
<b>DTR-2I</b>	363.2	193.9	80-30-10	236.1	75-25-10	9.8
<b>DTR-3I</b>	237.2	219.2	80-30-10	177.1	80-40-10	11.8

**Table S2** First-order rate constants of diatrizoate removal in electrochemical reduction ( $k_{\text{DTR,red}}$ ,  $\text{h}^{-1}$ ), initial rates of  $\text{I}^-$  release ( $i_{0,\text{I}}$ ,  $\mu\text{mol L}^{-1} \text{h}^{-1}$ ), diatrizoate removal efficiencies ( $E_{\text{f,DTR}}$ ) and deiodination efficiencies ( $E_{\text{f,I}}$ ) observed in the electrochemical reduction at bare and Pd nanoparticles-loaded graphite felt, performed with  $\text{N}_2$  purge and at pH 7.0. Coulombic efficiencies ( $\epsilon$ ) were calculated for 2.72 h of applied electrolysis time, using the measured consumed electrical charge ( $I^*t$ ). Values are expressed as means of two experiments, with their standard deviations.

$E_{\text{CAT}}$ , V vs SHE	$I^*t$ , Ah	$^a k_{\text{DTR,red}}$ , $\text{h}^{-1}$	$^b i_{0,\text{I}}$ , $\mu\text{mol L}^{-1} \text{h}^{-1}$	$E_{\text{f,DTR}}$ , %	$E_{\text{f,I}}$ , %	$\epsilon$ , %
<b>Bare graphite felt</b>						
-1.1	0.24±0.06	0.43±0.02	2.17	71.3±0.6	54.4±1.6	0.046±0.009
-1.3	0.33±0.02	0.59±0.02	2.70	81.7±0.1	58.1±1.5	0.039±0.001
-1.5	0.46±0.02	0.78±0.01	3.94	87.6±0.7	63.7±3.6	0.033±0.001
-1.7	0.66±0.04	0.88±0.15	5.10	90.6±3.6	66.6±2.1	0.024±0.001
-1.5 (DO=7.2 $\text{mg L}^{-1}$ )	0.50±0.06	0.40±0.02	2.51	65.4±1.7	61.2±2.2	0.022±0.002
-1.5 (10 mM NaCl)	0.38±0.07	0.86±0.01	5.60	90.1±2.7	75.9±2.5	0.052±0.007
-1.5 (pH=11)	0.36±0.03	1.03±0.02	5.97	94.0±0.3	71.7±0.6	0.052±0.003
-1.5 (200 $\text{mL min}^{-1}$ )	0.41±0.03	1.10±0.06	6.02	98.1±1.7	81.6±1.7	0.054±0.002
-1.7, <sup>c</sup> HWW	1.56±0.10	0.27±0.11	3.33	52.4±6.5	54.8±7.8	0.004±0.001
<b>Pd NP-graphite felt</b>						
-1.1	0.76±0.02	0.61±0.01	4.14	85.0±2.5	83.3±1.3	0.026±0.001
-1.3	0.88±0.05	0.71±0.01	6.05	87.3±3.1	92.5±0.9	0.025±0.002
-1.5	1.28±0.04	0.91±0.01	11.1	91.6±0.4	99.0±0.0	0.020±0.001
-1.7	1.84±0.07	1.07±0.02	11.5	94.7±1.4	99.0±0.6	0.014±0.001
-1.5 (DO=0 $\text{mg L}^{-1}$ )	1.33±0.02	0.73±0.09	9.25	86.6±2.7	93.4±0.6	0.017±0.001
-1.5 (10 mM NaCl)	1.44±0.11	1.50±0.04	13.9	98.6±0.8	97.6±0.5	0.018±0.002
-1.5 (pH=11)	1.12±0.04	0.72±0.04	5.23	87.4±3.0	83.2±0.2	0.018±0.001
-1.5 (200 $\text{mL min}^{-1}$ )	1.68±0.08	1.41±0.03	16.8	96.2±0.8	95.5±0.5	0.015±0.001
-1.7, HWW	2.48±0.08	0.32±0.03	4.20	60.0±2.7	88.5±0.6	0.006±0.001

<sup>a</sup> $r^2 \geq 0.985$ , <sup>b</sup> $i_{0,\text{I}}$  were calculated as the slope of the tangent line at  $t=0$  h of the curve of mean chloride ions concentration versus time. <sup>c</sup>HWW=hospital wastewater.

**Table S3** Characteristics of hospital wastewater. The values are presented as mean values of two measurements, with their standard deviations.

Parameter	Mean±Standard Deviation
DOC (mg L <sup>-1</sup> )	83.1±1.4
IC* (mg L <sup>-1</sup> )	156.0±0.1
Cl <sup>-</sup> (mg L <sup>-1</sup> )	769.3±3.2
SO <sub>4</sub> <sup>2-</sup> (mg L <sup>-1</sup> )	14.8±0.7
NH <sub>4</sub> -N (mg L <sup>-1</sup> )	62.6±2.4

\*IC=inorganic carbon